ChemComm

Accepted Manuscript

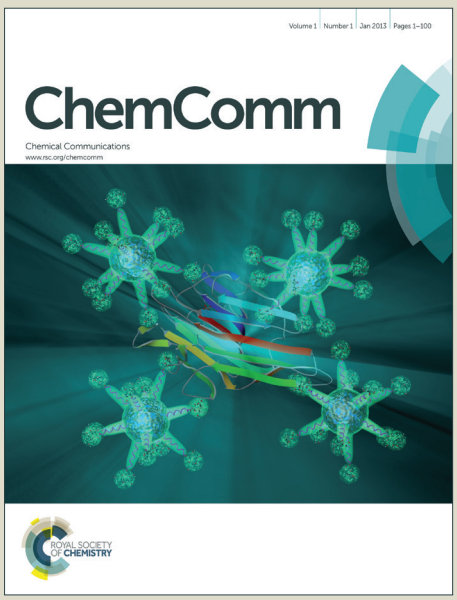

ROYAL SOCIETY OF CHEMISTRY

www.rsc.org/chemcomm

Journal Name

RSCPublishing

COMMUNICATION

Selective Oxidation of Veratryl Alcohol with Composites of Au Nanoparticles and Graphene Quantum Dots as Catalysts

Cite this: DOI: 10.1039/x0xx00000x

Received 00th January 2012,
Accepted 00th January 2012

DOI: 10.1039/x0xx00000x

www.rsc.org/

Xiaochen Wu[a], Shouwu Guo[a]* and Jingyan Zhang[b]*

Abstract Veratryl alcohol can be oxidized into veratryl aldehyde or veratric acid with excellent selectivity and efficient conversion under acidic and alkali conditions using Au nanoparticles and graphene quantum dots composites (Au/GQDs) as catalysts.

Veratryl alcohol (VA) has been often utilized as a model compound to study the reaction pathways of decomposition or chemical transformation of natural abounded lignin for the production of biofuels and aromatic chemicals.[1-3] VA could be selectively oxidized to veratryl aldehyde in the presence of catalysts including enzymes,[4] metal porphyrin complexes,[5, 6] cobalt(salen) complexes,[3, 7, 8] or zeolitic imidazolate frameworks etc.[9] However, the high cost and poor stability of the enzyme and small molecular catalysts severely impede their practical application. Having higher selectivity and less possibility to be deactivated by oxygen,[10] Au nanoparticles (NPs) supported on various matrices also have been employed to catalyze alcohol oxidation.[11] Recently, it has been reported that the Au NPs supported on carbonaceous materials exhibited higher catalytic activity, selectivity, and better environmental suitability than those attached onto other substrates, especially the commonly used metal oxides.[12-14] However, Au NPs centered catalysts are almost inactive in the absence of base or basic supports in many oxidation reactions.[15-17] We and others recently discovered that graphene quantum dots (GQDs) alone and the nanoarchitectures assembled with GQDs could dramatically improve the activity and stability of the catalysts, due to the synergetic effect raised by GQDs that possess excellent electron conductivity and good chemical/physical stabilities.[18, 19] On the basis of these findings, in this work we explored the catalytic properties of the composites of Au NPs and GQDs (abbreviated as Au/GQDs) in VA oxidation. As will be shown, with the Au/GQDs as catalysts, VA can be oxidized selectively into veratryl aldehyde or veratric acid using hydrogen peroxide with excellent yield and selectivity. Due to the good stability and high affinity to aromatic alcohols of the GQDs, and the strong interaction between Au NPs and GQDs, the Au/GQDs composites show a synergistically enhanced catalytic activity in VA oxidation, which is much higher that of Au NPs or GQDs.

The GQDs used in this work were fabricated through photo-Fenton reaction of graphene oxide as previously reported.[20, 21] The lateral sizes of GQDs range in 25-35 nm, and the average height of GQDs

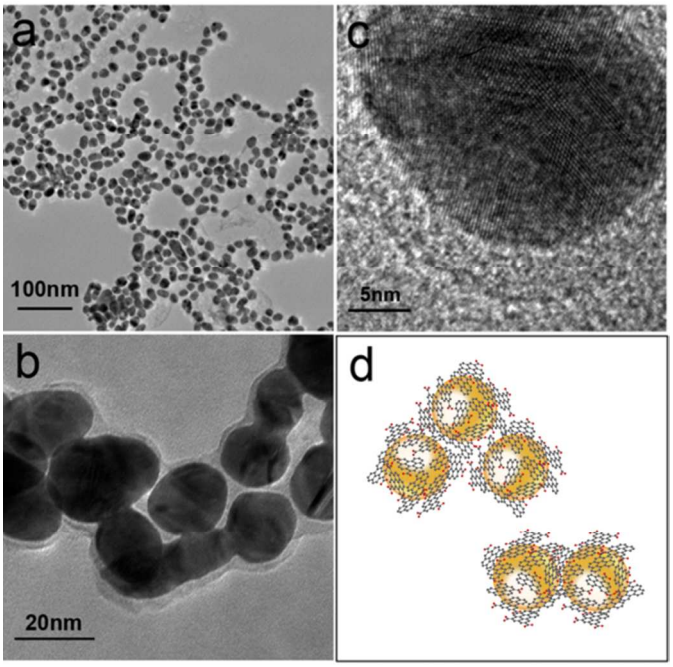

Figure 1. Structure of Au/GQDs composites. TEM images of the Au/GQDs composites: (a) overall images, (b) 5-fold magnification, and (c) 20-fold magnification. (d) Schematic representation of their structures.

is ~ 1 nm, revealing the single atomic layered feature (Figure S1). The Au/GQDs composites were prepared through a facile one-pot reaction using GQDs, $HAuCl_4$ and trisodium citrate as raw materials (detailed in the experimental part).[22] In contrast to the bare Au NPs prepared under the same condition (Figure S2), the TEM (transmission electron microscopy) images (Figure 1a, b) show that the Au NPs are coated by GQDs forming a core-shell structure in the Au/GQDs composites, which was further confirmed by the HRTEM (high resolution TEM) image as shown in Figure 1c (Figure S3). On the basis of TEM images, the structure of Au/GQDs is schematically

depicted in Figure 1d. To elaborate the chemical composition of Au/GQDs, Raman, FT-IR (Fourier transform infrared) and XPS (X-ray photoelectron spectroscopy) of Au/GQDs were acquired and compared with those of GQDs. As illustrated in Figure S4a, the ratio of D to G bands intensities in the Raman spectra of Au/GQDs (~ 0.855) is higher than that of bare GQDs (~ 0.825), indicating the partial reduction of GQDs. Additionally, by comparing the FT-IR spectra of Au/GQDs and GQDs, it can be noted that within the composites there are certain oxygen containing groups from GQDs, including epoxy, alkoxy, and carbonyl groups, but these groups are much less than that in the bare GQDs (Figure S4b).[23] It is possible that the oxygen containing groups on GQDs were reduced during the Au NPs formation due to the presence of trisodium citrate in the preparation. XPS data further confirmed this assumption. As depicted in Figure S3c and d, all of the C1s XPS peak intensities at 286.4, 287.8 and 288.5 eV, corresponding to C-O (epoxy and alkoxy), C=O (carbonyl) and COOH (carboxylic) groups in Au/GQDs composites, respectively, were decreased dramatically in comparing with those in bare GQDs. Owing to these oxygen containing groups can effectively prevent the Au NPs from aggregation, the as-obtained Au/GQDs composites exhibit much better dispensability and stability in aqueous solution than bare Au NPs.[20]

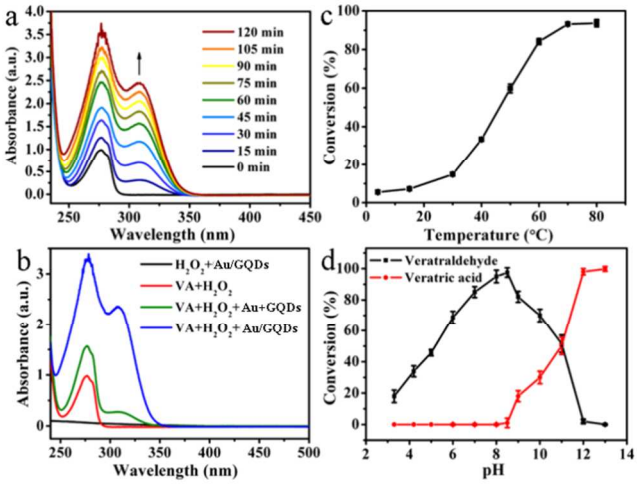

Figure 2. Oxidation of VA catalyzed by the Au/GQDs composites. (a) UV-vis spectra of the oxidation products of veratryl alcohol *versus* reaction time at pH 8.5. The experiments were carried out with 15 μg of Au/GQDs, 3 mM of H_2O_2 and 0.3 mM of VA at 50 °C; (b) The oxidation reaction of VA was carried out with different catalysts under the same condition for 2 h; (c) Conversion rates of VA catalyzed by the Au/GQDs at pH 8.5 with different reaction temperature for 1 h; (d) Conversion rates of VA catalyzed by the Au/GQDs at 50 °C for 2 h with varying pH.

To explore the catalytic activity of the as-obtained Au/GQDs composites, oxidation of VA using H_2O_2 as an oxidizing agent was employed as a model system. In a typical experiment, VA (0.3 μmol), H_2O_2 (3 μmol) was mixed with 15 μg of Au/GQDs composites in 1 mL of aqueous solution at 50 °C. The reaction was monitored with UV-vis spectroscopy. As shown in Figure 2a, after 15 min of the reaction, an absorption peak centered at 310 nm, corresponding to veratryl aldehyde,[24] could be detected clearly, and the peak intensity increased rapidly with the reaction time increased, indicating that the Au/GQDs and H_2O_2 could convert VA to veratryl aldehyde. The conversion percentage and selectivity of VA to veratryl aldehyde were analyzed using GC-MS quantitatively. As summarized in Table S1, after 2 h of the reaction, 97% of VA was converted to veratryl aldehyde, with above 99% selectivity. The detailed optimizations of the Au/GQDs and H_2O_2 in VA oxidation were summarized in Figure S5a and b. For comparison, the oxidation of VA with H_2O_2 in the presence of bare Au NPs, GQDs, and physical mixture of GQDs with Au NPs (GQDs + Au) were also carried out under the same conditions, respectively. Figure 2b shows that within 2 h of the reaction, only a small peak of veratryl aldehyde was observed using the mixture of GQDs and Au NPs as a catalyst (green line in Figure 2b). The Au/GQDs composites also exhibit great stability, they still maintain more than 80% activity after 6 cycles (Figure S5c).

The catalytic activity of Au NPs related catalysts depends strongly on temperature and the pH of the reaction system,[25-27] hence, these two factors of the reaction system with Au/GQDs as catalysts were also investigated. As illustrated in Figure 2c, the conversion of VA to veratryl aldehyde at 4 °C is less than 10%, but it can reach up to 90% at 70 °C (reaction time 1 h, pH 8.5). Apparently, high temperature is beneficial to the catalytic activity of the Au/GQDs. To examine the effect of pH on the catalytic activity of Au/GQDs, the reactions were performed under acidic and basic conditions, and the results were analyzed with GC-MS. As illustrated in Figure 2d, the Au/GQDs composites possess the catalytic ability even in pH 3.3 solution, and the conversion of VA to veratryl aldehyde was 17% within 2 h; when the reaction mixture is at pH 5, the conversion can reach up to 45% with extraordinary selectivity to veratryl aldehyde, and only about 30% of acid was formed after 21 h of reaction (Figure S6, Table S2). This result is different from many published works that the Au catalytic systems are inactive in the absence of base or basic supports.[15-17] In other words, the Au/GQDs can catalyze the oxidation of VA under acidic condition. This is important in lignin depolymerization, because the first step in the most currently used methods of depolymerization is acid treatment, which thus requires the subsequent used catalysts including enzymes have very high stability under acidic conditions. The stability and catalytic activity of the Au/GQDs under acidic condition may contributed by its out inert layer of GQDs on Au NPs (Figure 1).

When the pH value was further increased to above 7, the conversion of VA to veratryl aldehyde raised up quickly to more than 90% in 2 h of the reaction. Besides the veratryl aldehyde, veratric acid was also produced. The conversion of VA to veratric acid was further improved to more than 99%, when the pH of the reaction reaches to 13. Apparently, under the basic condition, the catalytic activity of the Au/GQDs was enhanced. In fact, VA was first converted to veratryl aldehyde, then to veratric acid under either basic or acidic conditions (Figure S6 and Table S2). These results indicate that with Au/GQDs catalysts, VA can be oxidized into veratraldehyde or veratric acid selectively by tuning the reaction time or pH (Table 1). For instance, under basic condition, only aldehyde was formed in a short time, while in a longer reaction time, such as 6.5 h (Table S2), only acid was obtained.

The high activity and selectivity of Au/GQDs may be contributed by GQDs, Au NPs, and probably their synergistic effect too. It was generally accepted that the residual oxygen-containing functional groups on the surface of supported Au catalysts play a key role in their catalytic performances, especially for the dehydrogenation and oxidization reactions.[28] The GQDs with plenty of the periphery carboxylic groups show high peroxidase-like activity under acidic environment.[29] That's possibly the reason why Au/GQDs composites exhibit catalytic activity under acidic condition, since Au NPs alone are inactive. In fact, graphene oxide (GO) was reported to enhance the chemiluminescence of luminol-H_2O_2 system in a weakly alkaline medium.[30] In luminol-H_2O_2 system, the GO functioned through the generation singlet oxygen $^1O_2$ intermediate. We thus infer that under acidic condition, $^1O_2$ is possibly involved in the

reaction catalyzed by the Au/GQDs. Reactions with the inhibitor of $^1O_2$ supported this assumption. As shown in Figure S7a, NaN_3 could effectively inhibit the reaction at pH 5. In addition, the reaction rate was enhanced when the reaction was carried out in D_2O instead of H_2O (Figure S7b), because the life time of $^1O_2$ is longer in D_2O than in H_2O.[31] Apparently, under alkali condition, $^1O_2$ was not, or only involved partially since the reaction was barely inhibited at pH 8.5 or 11 by NaN_3. To further confirm this conclusion, the reaction was monitored with $^1O_2$ trapping agents. As shown in Figure 3a, when $^1O_2$ trapping agent 2,2,6,6-tetramethylpiperidine (TEMP) was added to the mixture of Au/GQDs and H_2O_2, the signal of TEMP oxide (TEMPO) was detected, and the signal intensity was increased with the amount of Au/GQDs used. While in all control samples, only a very weak signal was observed possibly from impurity of the trace oxidized TEMP. Interestingly, the signal intensities are similar in the samples of different pH, suggesting that $^1O_2$ was present in all pH conditions. It is likely that singlet oxygen was converted from other active species under basic condition.[32]

Table 1. The results of VA oxidation at different pH using the Au/GQDs composites as catalysts for 24 h. Reaction conditions: 15 μg of Au/GQDs, 3 mM of H_2O_2, 0.3 mM of VA, 50 °C.

pH	Conversion (%)	Product selectivity (%)	
		Veratraldehyde	Veratric acid
2.5	34	>99	-
3	42	>99	-
4	59	>99	-
5	>99	66	34
6	>99	57	43
7	>99	51	49
8	>99	17	83
9	>99	2	98
10	>99	-	>99
11	>99	-	>99

Since under basic condition, singlet oxygen inhibitor cannot inhibit the oxidation reaction catalyzed by Au/GQDs, a superoxide anion trapping agent, disodium 4,5-dihydroxy-1,3-benzenedisulfonate (Tiron), was employed to examine the existence of superoxide anion. Strong signal of Tiron oxidation product was detected at pH above 7, but not below 7 (Figure 3b), confirming that superoxide anion was the active species under alkali condition. Interestingly, a weak signal of hydroxyl radical in alkali condition was also detected (Figure S8). However, the reaction cannot be inhibited by any hydroxyl radical quenchers, such as isopropanol and tert-butanol (Figure S9), suggesting that trace hydroxyl radical we observed was possibly converted from O^{-}_2. Especially under basic condition, H_2O_2 decomposes into O_2 very easily, which then reacts with GQDs forming O^{-}_2 that is more stable in high pH solution, similar to luminol-H_2O_2 with graphene oxide system.[30] The oxygen containing radical species involved in the catalytic oxidation reaction was also supported by the reaction with oxygen instead of H_2O_2, but the reaction with oxygen was less efficient (Figure S10).

The role of Au NPs apparently is not only a carrier of GQDs, because the activity of Au/GQDs is much higher than that of GQDs (Figure 2 and Table S1). We found that under different ratio of GQDs to Au NPs, the activities of the composites are different (Figure S11) suggesting that both of them contributed to the activity. Our previous work showed that GQDs could enhance nuclease activity of the copper complexes through efficient electron-transfer from the electron-rich GQDs to the copper complexes.[33] There may also exist interaction between Au NPs and GQDs, which enhances the activity of GQDs with H_2O_2, or increases the lifetime of active species. The assumption, however, need to be further proved. During the preparation of this manuscript, a paper showed that graphene covered on the Pt surface could promote Pt-catalyzed carbon monoxide oxidation was published online. The authors believed that graphene weakens the

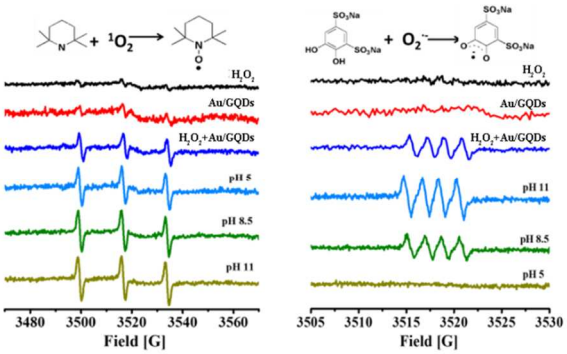

Figure 3. Catalytic active species generated by the Au/GQDs composites with H_2O_2. Left: EPR spectra of H_2O_2 +Au/GQDs (5 μg/mL) with singlet oxygen trapping agent TEMP (20 mM) at pH 5, 8.5 and 11. Controls are H_2O_2 (5 mM), Au/GQDs (2.5 μg/mL), and Au/GQDs (2.5 μg/mL) with H_2O_2 in the presence of TEMP at pH 5. Right: EPR spectra of Au/GQDs (10 μg/mL)+H_2O_2 with superoxide anion trapping agent Tiron (20 mM) at pH 11, 8.5, and 5. Controls are H_2O_2 (5 mM), Au/GQDs (5 μg/mL), and Au/GQDs (5 μg/mL) with H_2O_2 in the presence of Tiron at pH 11.

strong interaction between carbon monoxide and Pt, consequently facilitates the CO oxidation with lower apparent activation energy based on density function calculation.[34] Importantly, we found that Au/GQDs composites are almost inactive to the oxidization of primary aliphatic alcohols with H_2O_2. As shown in Table S3, under the same reaction condition, only trace aldehydes were detected with aliphatic alcohols, including cyclohexane methanol, 4-methylcyclohexane methanol, 1-hexanol and 1-pentanol. Differently, the aromatic alcohols, such as benzyl alcohol, 4-methylbenzyl alcohol, 4-methoxybenzyl alcohol, and cinnamyl alcohol were oxidized to the corresponding aldehydes or acids with pronounced conversion rates. Since the molecules with aromatic structural unit interact easily with GQDs through π-π stacking,[35] the large aromatic basal plane of GQDs in Au/GQDs thus absorbs the aromatic reactant, which then is easily oxidized by the active oxygen species generated *in situ* by GQDs with H_2O_2. The confinement of the aromatic reactants by GQDs accelerates their oxidation, in which Au NPs apparently are involved. This result may be similar to the palladium on graphene catalytic system.[36] While for aliphatic alcohols, their hydrophobic tail is unfavorable to the interaction with GQDs, thus cannot be efficiently oxidized by the active species generated by Au/GQDs with H_2O_2. The mechanism of the oxidation reaction catalyzed by Au/GQDs was thus summarized in Scheme 1. Through π-π stacking, VA was absorbed on the Au/GQDs, the active species singlet oxygen primarily generated by GQDs with H_2O_2 under acidic condition oxidize reactant; the superoxide anion and trace singlet oxygen generated by both Au

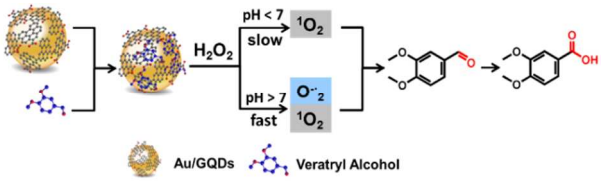

Scheme 1. Schematic illustration of possible mechanism for VA oxidation with Au/GQDs as catalysts at different pH.

NPs and GQDs with H_2O_2 oxidize the reactant under alkali condition, thus the reaction is faster. The excellent selectivity and conversion efficiency of the oxidation catalyzed by Au/GQDs are contributed by each components and their interaction.

Conclusions

In summary, we demonstrated that using the as-synthesized Au/GQDs composites as catalysts, VA can be oxidized into veratryl aldehyde or veratric acid by H_2O_2 with excellent selectivity and conversion efficiency through tuning the pH and reaction time. Inhibition reactions and EPR trapping experiments show that under acidic condition, singlet oxygen species that generated by GQDs with H_2O_2 play a critical role; while under alkali condition, both GQDs and Au NPs contributed to the oxidation using superoxide anion and trace singlet oxygen species generated by GQDs and Au with H_2O_2. In addition, the large aromatic basal plane of GQDs in the Au/GQDs composite makes it as an efficient catalyst selectively for aromatic alcohols' oxidation. With the excellent catalytic performance and stability, we envisage that Au/GQDs could find potential applications in alcohols oxidation, such as lignin oxidation.

Notes and references

* Corresponding authors
[a] Department of Electronic Engineering, School of Electronic Information and Electrical Engineering, Shanghai Jiao Tong University, Shanghai 200240, P. R. China.
[b]State Key Laboratory of Bioreactor Engineering, Shanghai Key Laboratory of New Drug Design, School of Pharmacy, East China University of Science and Technology, Shanghai, 200237, P. R. China.
Email: swguo@sjtu.edu.cn; jyzhang@ecust.edu.cn.

Electronic Supplementary Information (ESI) available: Experimental procedures, additional TEM, Raman, FT-IR, XPS data of the Au/GQDs, UV and EPR spectra of the reaction product and reaction intermediates are included in the supporting information. See DOI: 10.1039/c000000x/

Acknowledgements

This research was carried out with financial support from the National Science Foundation of China (No. 11374205), the state key laboratory of bioreactor engineering (No. 2060204), 111 Project (No. B07023), the Shanghai Committee of Science and Technology (Nos. 11DZ2260600 and 12nm0503500), national "973 Program" of China (No. 2014CB260411), and national "863" Program of China (No. 2012AA022603).

1. J. Zakzeski, P. C. A. Bruijnincx and B. M. Weckhuysen, *Green Chem.*, 2011, **13**, 671-680.
2. H. Fan, Y. Yang, J. Song, G. Ding, Congyi Wu, G. Yang and B. Han, *Green Chem.*, 2014, **16**, 600-604.
3. K. Kervinen, H. Korpi, M. Leskelä and T. Repo, *J. Mol. Catal. A-Chem.*, 2003, **203**, 9-19.
4. M. Díaz-González, T. Vidal and T. Tzanov, *Appl. Microbiol. Biotechnol.*, 2011, **89**, 1693-1700.
5. W. Zhu and W. T. Ford, *J. Mol. Catal.*, 1993, **78**, 367-378.
6. F. Cui and D. Dolphin, *Can. J. Chem.*, 1992, **70**, 2314-2318.
7. K. Kervinen, M. Allmendinger, M. Leskela¨, T. Repo and B. Rieger, *Phys. Chem. Chem. Phys.*, 2003, **5**, 4450-4454.
8. V. Sippola, O. Krause and T. Vuorinen, *J. Wood Chem. Technol.*, 2004, **24**, 323-340.
9. J. Zakzeskia, A. D¸ebczak, P. C. A. Bruijnincx and B. M. Weckhuysen, *Appl. Catal. A-Gen.*, 2011, **394**, 79-85.
10. X. Yu, Y. Huo, J. Yang, S. Chang, Y. Ma and W. Huang, *Appl. Surf. Sci.*, 2013, **280**, 450- 455.
11. C. D. Pina, E. Falletta and M. Rossi, *Chem. Soc. Rev.*, 2012, **41**, 350-369.
12. S. Demirel, P. Kern, M. Lucas and P. Claus, *Catal. Today*, 2007, **122**, 292-300.
13. E. G. Rodrigues, S. A. C. Carabineiro, J. J. Delgado, X. Chen, M. F. R. Pereira and J. J. M. Órfão, *J. Catal.*, 2012, **285**, 83-91.
14. J. L. Figueiredo and M. F. R. Pereira, *Catal. Today*, 2010, **150**, 2-7.
15. T. Mallat and A. Baiker, *Chem. Rev.*, 2004, **104**, 3037-3058.
16. S. Carrettin, P. McMorn, P. Johnston, K. Griffin, C. J. Kiely and G. J. Hutchings, *Phys. Chem. Chem. Phys.*, 2003, **5** 1329-1336.
17. D. I. Enache, D. W. Knight and G. J. Hutchings, *Catal. Lett.*, 2005, **103**, 43-52.
18. X. Zhou, Z. Tian, J. Li, H. Ruan, Y. Ma, Z. Yang and Y. Qu, *Nanoscale*, 2014, **6**, 2603-2607.
19. D. Pan, C. Xi, Z. Li, L. Wang, Z. Chen, B. Lu and M. Wu, *J. Mater. Chem. A*, 2013, **1**, 3551-3555.
20. X. Zhou, Y. Zhang, C. Wang, X. Wu, Y. Yang, B. Zheng, H. Wu, S. Guo and J. Zhang, *ACS Nano*, 2012, **6**, 6592-6599.
21. X. Zhou, J. Zhang, H. Wu, H. Yang, J. Zhang and S. Guo, *J. Phys. Chem. C*, 2011, **115**, 11957-11961.
22. X. Ji, X. Song, J. Li, Y. Bai, W. Yang and X. Peng, *J. Am. Chem. Soc.*, 2007, **129**, 13939-13948.
23. J. Zhang, H. Yang, G. Shen, P. Cheng, J. Zhang and S. Guo, *Chem. Commun.*, 2010, **46**, 1112-1114.
24. G. I. Panoutsopoulos and C. Beedham, *Acta Biochim. Pol.*, 2004, **51**, 649-663.
25. J. Zhu, J. L. Figueiredo and J. L. Faria, *Catal. Commun.*, 2008, **9**, 2395-2397.
26. L. Yan, T. Zhang, W. Lei, Q. Xu, X. Zhou, P. Xu, Y. Wang and G. Liu, *Catal. Today*, 2014, **224**, 140-146.
27. S. K. Klitgaard, A. T. D. Riva, S. Helveg, R. M. Werchmeister and C. H. Christensen, *Catal. Lett.*, 2008, **126**, 213-217.
28. J. Zhu, S. A. C. Carabineiro, D. Shan, J. L. Faria, Y. Zhu and J. L. Figueiredo, *J. Catal.*, 2010, **274**, 207-214.
29. Y. Zhang, C. Wu, X. Zhou, X. Wu, Y. Yang, H. Wu, S. Guo and J. Zhang, *Nanoscale*, 2013, **5**, 1816-1819.
30. D. M. Wang, Y. Zhang, L. L. Zheng, X. X. Yang, Y. Wang and C. Z. Huang, *J. Phys. Chem. C*, 2012, **116**, 21622-21628.
31. W. R. Haag and J. Hoigne, *Environ. Sci. Technol.*, 1986, **20**, 341-348.
32. r. Edwin Welles Kellogg and I. Fridovich, *J. Biol. Chem.*, 1975, **250**, 8812-8817.
33. B. Zheng, C. Wang, X. Xin, F. Liu, X. Zhou, J. Zhang and S. Guo, *J. Phys. Chem. C*, 2014, **118**, 7637-7642.
34. Y. Yao, Q. Fu, Y. Y. Zhang, X. Weng, H. Li, M. Chen, L. Jin, A. Dong, R. Mu, P. Jiang, L. Liu, H. Bluhm, Z. Liu, S. B. Zhang and X. Bao, *Proc. Natl. Acad. Sci. U. S. A.*, 2014, **111**, 17023-17028.
35. Z. Liu, J. T. Robinson, X. Sun and H. Dai, *J. Am. Chem. Soc.*, 2008, **130**, 10876-10877.
36. G. Wu, X. Wang, N. Guan and L. Li, *Appl. Catal. B-Environ.*, 2013, **136-137**, 177-185.

